Shilnikov homoclinic orbit bifurcations in the Chua's circuit

R. O. Medrano-T.
Instituto de Física, Universidade de São Paulo, Caixa Postal 66318, 05315-970 São Paulo, Brazil

M. S. Baptista
Universität Potsdam, Institut für Physik, Am Neuen Palais 10, D-14469 Potsdam, Germany

I. L. Caldas
Instituto de Física, Universidade de São Paulo, Caixa Postal 66318, 05315-970 São Paulo, Brazil

(Received 20 May 2006; accepted 31 October 2006; published online 7 December 2006)

We analytically describe the complex scenario of homoclinic bifurcations in the Chua's circuit. We obtain a general scaling law that gives the ratio between bifurcation parameters of different nearby homoclinic orbits. As an application of this theoretical approach, we estimate the number of higher order subsidiary homoclinic orbits that appear between two consecutive lower order subsidiary orbits. Our analytical finds might be valid for a large class of dynamical systems and are numerically confirmed in the parameter space of the Chua's circuit. © *2006 American Institute of Physics*. [DOI: 10.1063/1.2401060]

Shilnikov homoclinic orbits are trajectories that depart from a fixed saddle-focus point, with specific eigenvalues, and return to it after an infinite amount of time (that is also true to time reversal evolution). That results in an orbit that is unstable and has an infinite period. These two main characteristics contribute in the hardness for its observation in a dynamical system as well as in nature. However, its presence reveals fundamental characteristics of the system involved, as the existence of unstable periodic orbits embedded in a chaotic set. Once the unstable periodic orbits give invariants quantities of this set,[1] the Shilnikov homoclinic orbits are also related to the characteristics of the chaotic set. Their connection with the fundamental dynamical properties is verified in a wide variety of systems. A series of numerical and experimental investigations reveal how Shilnikov homoclinic orbits, in the vicinity of a chaotic attractor, determine its dynamical and topological properties.[4] Thus, the Shilnikov orbits are related to the returning time of the trajectory of a CO_2 laser,[5] also to the topology of a glow-discharge system.[6] Moreover, some class of spiking neurons are modeled by chaos governed by such orbits,[7,8] and their presence are connected to the intermittence present in rabbit arteries.[9] These orbits are shown to be behind the mechanism of noise-induced phenomena,[10] and they are also responsible for the dynamics of an electrochemical oscillator.[11] In this work, we contribute to the understanding of how Shilnikov homoclinic orbits appear on the parameter space of systems as the ones above mentioned, by showing that these orbits are not only distributed following an universal rule but also exist for large parameter variations. We then confirm our previsions in the Chua's circuit system.[12]

I. INTRODUCTION

The relation between homoclinic orbits and the existence of a complex dynamical behavior was first noticed by Poincaré, who studied the solvability of the equations of the three-body problem in the end of the 19th century. He showed the nonintegrability of them due to the existence of homoclinic orbits which cause the appearance of sensitivity to initial conditions. Then, in the sixties, Smale showed that chaos in a discrete chaotic system implies the existence of these orbits.[2] Soon later, for a three-dimensional class of continuous systems, Shilnikov[3] showed that the existence of a Shilnikov homoclinic orbit, defined as the joint of the stable and unstable manifolds of a saddle-focus fixed point, with specific eigenvalues,[13] implies the existence of a horseshoe in the neighborhood of this orbit, and therefore, chaos.[2]

The existence of only one Shilnikov homoclinic orbit is already sufficient to introduce a high degree of complexity in a dynamical system. One-parameter local bifurcation analysis, in the neighborhood of a Shilnikov homoclinic orbit, shows that there exists an infinite number of other homoclinic orbits.[14–18] Similar analysis with the same considerations have been done for complex trajectories with a high number of loops.[19,20] Since each orbit is associated with a horseshoe, in the neighborhood of one homoclinic orbit, there is an infinite number of chaotic sets.

In this context, it is important to localize the homoclinic orbits in the parameter space, and to determine the structure by which homoclinic orbits appear in this space. This knowledge indicates the place of chaos and bifurcations of attractors in the parameter space and may help to understand the relation between Shilnikov orbits and attractor bifurcations, as done, for example, in Ref. 21 for the Rössler system.

In a parameter neighborhood of a homoclinic orbit, regarded as H_j, there is a series of homoclinic bifurcations which creates subsidiary orbits, regarded as H_{nj}, that are topologically equivalent to H_j. Following the traditional terminology, we say that a homoclinic bifurcation happens for some parameter if there is a homoclinic orbit for this parameter. Given a primary homoclinic orbit of any j order (H_j) (the order of the orbit labels its topology), we analytically derive a scaling law that governs parameter distributions and

accumulations, i.e., a one-parameter approach of order nj subsidiary orbits (H_{nj}) into order $(n-1)j$ orbits $[H_{(n-1)j}]$, in the vicinity of a primary H_j ($n,j \in \mathbb{N}$ with $n \geqslant 2$ and $j \geqslant 1$). This is an extension of previous results obtained by Gaspard[18] relating critical parameters of the accumulation of the subsidiary H_2 into the primary H_1 homoclinic orbit. Our derivation extends the one presented in Ref. 18 including not only the accumulation of the subsidiary H_2 orbit into the primary H_1 orbit but also the distributions of any subsidiary H_{nj}. Our results also agree with the work of Feroe,[19] that shows that one H_4 subsidiary homoclinic orbit in the neighborhood of a H_2 subsidiary has the same topology as the H_2, and not of the H_1; therefore, one can consider the subsidiary H_2 to be a primary orbit. By showing that subsidiaries accumulate into a subsidiary in the same way that subsidiaries accumulate into a primary, we are led also to the same conclusion: a subsidiary can be thought of as a primary with a set of subsidiary orbits that accumulates into it. The new point in our work, as in the comparison with the results in Ref. 19 is that our verification is based not only on the existence of orbits H_{2n}, topologically similar to H_n, but in the existence of families of subsidiaries H_{2nj} that accumulate into subsidiaries H_{nj}. In addition, we show that all sets of homoclinic orbits H_{lnj} are distributed near H_{nj} following the same scaling laws. Moreover, we also estimate the number of subsidiary H_{nj} that appear between two consecutive subsidiary orbits $H_{(n-1)j}$, in the vicinity of the primary orbit H_j.

As pointed out in Ref. 22, it is impossible to analytically describe completely the parameter space structure of homoclinic orbit bifurcations of three-dimensional systems with homoclinic tangencies. On the other hand, our work shows that we can understand very well the bifurcations in the vicinity of the primary orbits, which appear in extended regions of the parameter space. As a direct application of the proposed theoretical approach, we accurately described the bidimensional parameter space of the homoclinic orbit bifurcations in the Chua's circuit, in the vicinity of the primary orbits.[23] This parameter space is not completely new, because it was already partially drawn in Ref. 24, in which a few orbits can be observed. In the present work, though, we show its microscopic structure, by revealing the scaling at which subsidiary homoclinic orbits appear in extended regions of the parameter space. Therefore, an experimentalist that intends to reproduce our results has the flexibility of finding homoclinic orbits (and the proposed scaling) using parameters that are accessible from the experiment, and it is not restricted to any special parameter condition. The choice of this circuit is grounded in the following facts: (i) it is a system that has Shilnikov orbits, fact explored to demonstrate that this circuit is chaotic;[25] (ii) we have already developed an accurate reliable method to determine homoclinic orbits in piecewise systems,[26] like the Chua's circuit; (iii) since this circuit is being widely used to demonstrate experimentally properties of chaotic systems, we expect that the results shown here could be quickly experimentally reproduced.

This work is organized as follows: In Sec. II, we present the theoretical description for the bifurcation of the homoclinic orbits, i.e., the proof that there is an infinite number of homoclinic orbits and the derivation of the scaling law, the rule by which these orbits appear in the parameter space. In Sec. II A, we estimate the number of subsidiary homoclinic orbits that appear between two consecutive subsidiary orbits. In Secs. III and III A, we present the numerically obtained scenario of homoclinic bifurcations in the Chua's circuit and we show the outstanding agreement between the introduced theory and the numerical results. Finally, in Sec. IV are the conclusions.

II. SCENARIO OF HOMOCLINIC ORBITS BIFURCATIONS

Let us derive the scaling of the appearance of homoclinic orbits in dynamical systems that can be reduced to the following normal form:[17]

$$\begin{aligned} \dot{x} &= \rho x - \omega y + P(x,y,z;\mu) \\ \dot{y} &= \omega x + \rho y + Q(x,y,z;\mu) \\ \dot{z} &= \lambda z + R(x,y,z;\mu) \end{aligned} \tag{1}$$

where the eigenvalues of the saddle-focus fixed points are $\lambda_1=\lambda$ and $\lambda_{2,3}=\rho \pm i\omega$, with $\lambda\rho<0$ and $\omega \neq 0$. The functions P, Q, and R are real, analytics, and vanish with their first derivatives for the fixed point in the origin. μ is a control parameter.

Theorem 1: *If there is a primary homoclinic orbit H_j with order j for the parameter μ_j and the Shilnikov relation $|\rho/\lambda|<1$ is satisfied, there is an infinite number of subsidiary homoclinic orbits H_{nj}^i for the parameters μ_{nj}^i in the neighborhood of μ_j distributed in the parameter space with the ratio*

$$\lim_{i\to\infty}\left(\frac{\mu_{nj}^i - \mu_{nj}^{i+1}}{\mu_{nj}^{i-1} - \mu_{nj}^i}\right) = e^{-\lambda\pi/\omega},$$

where $i \in \mathbb{N}$ denotes the ith subsidiary homoclinic orbit of order nj.

The studies in Refs. 16, 18, and 19 have shown that a C^1 linearization of Eq. (1) is enough to investigate homoclinic orbits bifurcations. So, to prove Theorem 1, we will consider the first order terms of the Taylor development near the saddle-focus around the parameter μ_j for which a primary homoclinic orbit H_j exists. However, to observe other types of bifurcations, as for example, bifurcations of periodic orbits close to a saddle-focus point, one should consider higher order expansions as in Ref. 27.

In Fig. 1, we show an order-2 homoclinic orbit (H_2), a solution of Eq. (1), in the coordinates of the eigenvectors of the saddle-focus point. We define two surfaces, $\Sigma_0 = \{(x,y,z)|x^2+y^2 < \tilde{r}^2, z=h\}$ and $\Sigma_1 = \{(x,y,z)|y=0\ ,0<x<\tilde{r}, 0<z<h\}$, also represented in this figure by the dark gray and light gray regions, respectively. The number n of times that the trajectory is mapped from Σ_0 to Σ_1 gives the order of the homoclinic orbits. In the region within the cylinder containing these surfaces, the dynamics of Eqs. (1) is given by its linearized form around the saddle-focus point $(x,y,z)=(0,0,0)$. That is $(r,\theta,z)=(r_0e^{-\rho t}, \theta_0+\omega t, z_0e^{\lambda t})$ in

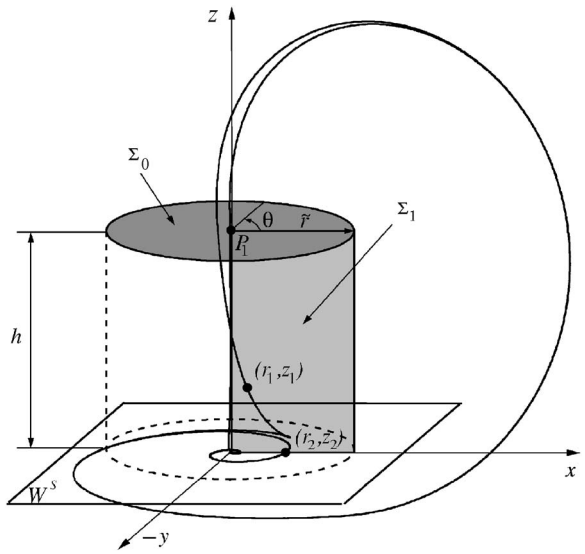

FIG. 1. An H_2 homoclinic orbit in the coordinates of the eigenvectors of the saddle-focus point ($x=y=z=0$). We show the surface Σ_0 on the top of the cylinder at $z=h$ and the surface Σ_1 at $y=0$. $P_1=(0,0,h)$ is the point that the unstable manifold of the saddle-focus point crosses the first time the plane Σ_0. (r_1,z_1) and (r_2,z_2) are successive points on Σ_1 mapped from Σ_0. W^S is the surface of the stable manifold nearby the saddle-focus point.

cylindrical coordinates. Note that an initial condition, inside the cylinder at $z=z_0$, needs a time $t=1/\lambda \ln h/z_0$ to cross Σ_0. Thus, the map $\psi^0:\Sigma_1\to\Sigma_0$ is obtained by

$$\psi^0(r_0,0,z_0)=\left(r_0\left(\frac{z_0}{h}\right)^{\rho/\lambda},\gamma,h\right),$$

with $\gamma=\omega/\lambda \ln h/z_0$ and $\theta_0=0$.

Let us assume that there is a primary homoclinic orbit H_1 for the parameter μ_1. The point $P_1=(0,0,h)$ is mapped from Σ_0 to Σ_1 to the point $(r_{H_1},0,0)$. We also assume that for a parameter μ close enough to μ_1, a point in Σ_0 close enough to P_1 is mapped nearby $(r_{H_1},0,0)$ by the map $\psi^1:\Sigma_0\to\Sigma_1$. So, we may consider the map ψ^1 a first order Taylor expansion around the point $(r_{H_1},0,0)$ in Σ_1. If one wants to consider higher order terms in this expansion one should follow the works in Ref. 28. However, for the accurate description of the homoclinic bifurcations in the Chua's circuit, the linear expansion is sufficient.

Putting this expansion in cylindrical coordinates, we arrive at

$$\psi^1(r_0,\theta_0,h)=(r_{H_1}+a\Delta\mu_1+pr_0\cos(\theta_0+\varphi_1),0,m\Delta\mu_1 + qr_0\cos(\theta_0+\varphi_2)),$$

where $\Delta\mu_1=\mu-\mu_1$, r_{H_1} represents the coordinate r of the first crossing of H_1 with the surface Σ_1, and the arbitrary constants a, m, p, q, φ_1, and φ_2 depend on the flow and they are not relevant for the scaling in Theorem 1. Note that for $\psi^1(0,0,h)$ with $\mu=\mu_1$ we obtain $(r_{H_1},0,0)$, which is the position of H_1 in Σ_1.

Applying $\psi^1\psi^0(r_0,0,z_0)$ we obtain a bidimensional map $\psi:\Sigma_1\to\Sigma_1$ given by

$$(r,z)=\left(r_{H_1}+a\Delta\mu_1+pr_0\left(\frac{z_0}{h}\right)^{\rho/\lambda}\cos(\gamma+\varphi_1),m\Delta\mu_1 + qr_0\left(\frac{z_0}{h}\right)^{\rho/\lambda}\cos(\gamma+\varphi_2)\right).$$

Here z is the vertical axis that contains P_0 and P_1, and r is the distance between a point in Σ_1 and this axis.

To obtain an order-n homoclinic orbit in the vicinity of a primary H_1, we have first to determine the points where the unstable manifold crosses Σ_1. The first point (r_1,z_1) is obtained by $\psi^1(P_1)=(r_{H_1}+a\Delta\mu_1,m\Delta\mu_1)$. The second point (r_2,z_2) is obtained by $\psi^2(P_1)=\psi\psi^1(P_1)$, the third by $\psi^3(P_1)=\psi\psi\psi^1(P_1)$ and the nth point (r_n,z_n) is obtained by $\psi^n(P_1)$:

$$\begin{pmatrix}r_n\\ z_n\end{pmatrix}=\begin{pmatrix}r_1+pr_{n-1}\left(\frac{z_{n-1}}{h}\right)^{\rho/\lambda}\cos(\gamma_{n-1})+\varphi_1\\ z_1+qr_{n-1}\left(\frac{z_{n-1}}{h}\right)^{\rho/\lambda}\cos(\gamma_{n-1})+\varphi_2\end{pmatrix},\quad n>1,$$

where $\gamma_{n-1}=\omega/\lambda \ln h/z_{n-1}$.

Generalizing this result to obtain an order-nj subsidiary homoclinic orbit H_{nj} in the vicinity of an order-j primary homoclinic orbit H_j, the point (r_{nj},z_{nj}) is obtained by $\psi^{nj}(P_1)$:

$$\begin{pmatrix}r_{nj}\\ z_{nj}\end{pmatrix}=\begin{cases}\begin{pmatrix}r_{H_j}+a\Delta\mu_j\\ m\Delta\mu_j\end{pmatrix}, & n=1\\ \begin{pmatrix}r_j+pr_{(n-1)j}\left[\frac{z_{(n-1)j}}{h}\right]^{\rho/\lambda}\cos[\gamma_{(n-1)j}+\varphi_1]\\ z_j+qr_{(n-1)j}\left[\frac{z_{(n-1)j}}{h}\right]^{\rho/\lambda}\cos[\gamma_{(n-1)j}+\varphi_2]\end{pmatrix}, & n>1\end{cases}\tag{2}$$

where $\Delta\mu_j=\mu-\mu_j$, and r_{H_j} represents the coordinate r of the jth crossing of H_j with the surface Σ_1. $j\geq 1$ is the order of the primary homoclinic orbit, and nj is the order of the subsidiary orbits with $n\geq 2$. Also, $\gamma_{(n-1)j}=\omega/\lambda \ln h/z_{(n-1)j}$ and the constants λ, ρ, and ω are associated to the eigenvalues of the fixed point of the primary homoclinic orbit H_j.

Having determined the points r_{nj}, the condition for the existence of any homoclinic orbit H_{nj} is $z_{nj}=0$,[29] what implies that

$$-z_j=qr_{(n-1)j}\left[\frac{z_{(n-1)j}}{h}\right]^{\rho/\lambda}\cos[\gamma_{(n-1)j}+\varphi_2].\tag{3}$$

To ensure the existence of a solution in Eq. (3) note that in the limit $z_{(n-1)j}\to 0$ the dominant terms are z_j, on the left-hand side, and $[z_{(n-1)j}]^{\rho/\lambda}$, on the right-hand side. From Eqs. (2) we can see that $z_j\leq[z_{(n-1)j}]_{\mathrm{MAX}}$, where $[z_{(n-1)j}]_{\mathrm{MAX}}$ means the maximal amplitude of $z_{(n-1)j}$. When the Shilnikov condition $|\rho/\lambda|<1$ is satisfied, in the limit $z_{(n-1)j}\to 0$, $z_j<[z_{(n-1)j}]^{\rho/\lambda}_{\mathrm{MAX}}$, which guarantees that the amplitude of the term containing the cosine function decreases slower than the value of z_j. For $z_{(n-1)j}\to 0$, the phase of the cosine function goes to infinity, which implies that there are an infinite

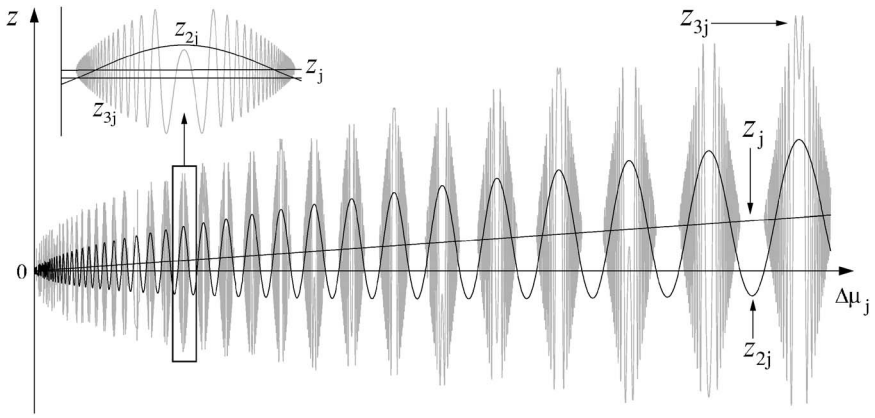

FIG. 2. Distribution of homoclinic orbit parameters μ_{2j} into μ_j and μ_{3j} into μ_{2j}. The curves gives the coordinate z_{nj} of the unstable manifold intersections with the surface Σ_1 [given by the solutions terms of Eqs. (2)] for $n=1$, 2, 3, in terms of $\Delta\mu_j=\mu-\mu_j$. Each $z_{nj}=0$ gives $\mu=\mu_{nj}$, the critical parameter of a homoclinic orbit H_{nj}, for the chosen parameters $r_{H_j}=1$, $a=0.1$, $m=1$, $p=1$, $q=0.1$, $\rho=1$, $\lambda=2$, $\omega=100$, $\phi_1=1$, $\phi_2=1$ and $h=0.1$. We show $\Delta\mu_j=\mu-\mu_j$. In the inset is a magnification of the box.

number of solutions for $z_{nj}=0$, as $z_j\to 0$. Therefore, the Shilnikov condition implies the existence of an infinite number of arbitrary order-nj homoclinic orbits with $\Delta\mu_j\neq 0$, in the vicinity of H_j. This is always true whenever all the conditions imposed by the Shilnikov Theorem are satisfied.

In Fig. 2 we illustrate the z_{nj} solutions of Eqs. (2), for $n=1$, $n=2$, and $n=3$, in the neighborhood of μ_j where the constants a, m, p, q, φ_1, and φ_2 were adjusted such that we can have a good visualization of the parameter space. We show z_j, z_{2j}, and z_{3j} with respect to $\Delta\mu_j=\mu-\mu_j$. The homoclinic orbits H_{2j} and H_{3j} exist whenever the coordinates z_{2j} and z_{3j} are equal to zero, respectively. And for $\Delta\mu_j=0$, H_j exists. An important fact in this picture is the similarity of the distribution of orbits between the finite number of H_{3j} near H_{2j} (see the inset in Fig. 2) and the infinite number of H_{2j} accumulating into H_j, for $\Delta\mu_j\to 0$. Also, in the parameter interval $\Delta\mu_j$ with a negative z_{nj}, there is not any homoclinic orbit. Note that there are infinite solutions of $z_{3j}=z_j$ accumulating into the parameter μ_{2j} [see the solution of z_{nj} with $n=3$ in Eqs. (2)], and that lead to a distribution of finite parameter values μ_{3j} (for which H_{3j} homoclinic orbits exist) that appear close to the parameters μ_{2j} (for which H_{2j} homoclinic orbits exist). In this sense we say that μ_{nj} (H_{nj}) is approaching into $\mu_{(n-1)j}$ ($H_{(n-1)j}$).

We introduce an upper index i to identify the many homoclinic orbits H^i_{nj} appearing in the parameter vicinity of $H_{(n-1)j}$. For $\Delta\mu_j\to 0$, given two consecutive homoclinic orbits that appear for the parameters μ^i_{nj} and μ^{i+1}_{nj}, the parameter difference $|\mu^i_{nj}-\mu_{(n-1)j}|$ decreases as i grows. The sequence for which orbits appear satisfies $|\mu^i_{nj}-\mu_{(n-1)j}|>|\mu^{i+1}_{nj}-\mu_{(n-1)j}|$. In the limit of $z_j\to 0$, Eq. (3) leads to $\phi^{i+1}-\phi^i=\pi$ for two consecutive solutions, where $\phi^i=\gamma^j_{(n-1)j}+\varphi_2$ is the phase of the solution i ($z^i_{nj}=0$) and $\phi^{i+1}=\gamma^{j+1}_{(n-1)j}+\varphi_2$, the phase for the consecutive solution $i+1$ ($z^{i+1}_{nj}=0$). Thus whenever the Shilnikov condition $|\rho/\lambda|<1$ is satisfied, we arrive at

$$\frac{z^{i+1}_{(n-1)j}}{z^i_{(n-1)j}}=e^{-\lambda\pi/\omega}. \tag{4}$$

In Eqs. (2) z_{nj} has a smooth solution if $z_{(n-1)j}>0$ [$z_{(n-1)j}<0$, z_{nj} does not have a solution]. Thus, we conclude that $d/d\Delta\mu_j z_{(n-1)j}=-d/d\mu z_{(n-1)j}\simeq$ const. in a neighborhood for which $\mu^i_{nj}-\mu^{i+1}_{nj}$ is small, as we can see in the inset of Fig. 2. Thus, $z^i_{(n-1)j}-z^{i+1}_{(n-1)j}/\mu^i_{nj}-\mu^{i+1}_{nj}=z^{i-1}_{(n-1)j}-z^i_{(n-1)j}/\mu^{i-1}_{nj}-\mu^i_{nj}$. Equation (4) implies that $z^i_{(n-1)j}-z^{i+1}_{(n-1)j}/z^{i-1}_{(n-1)j}-z^i_{(n-1)j}=e^{-\lambda\pi/\omega}$. So, finally, we arrive at the result announced by Theorem 1,

$$\lim_{i\to\infty}\left(\frac{\mu^i_{nj}-\mu^{i+1}_{nj}}{\mu^{i-1}_{nj}-\mu^i_{nj}}\right)=e^{-\lambda\pi/\omega}. \tag{5}$$

Note that the limit $i\to\infty$ is obtained for $z_j\to 0$, i.e., $\Delta\mu_j\to 0$. So, in this limit, for $n=2$, we have the accumulation of the subsidiaries H_{2j} into the primary H_j. Considering the primary homoclinic orbit parameter $\mu_j=0$, for $j=1$ and $n=2$, Eq. (5) describes the countable set of H_2 as shown in Refs. 16 and 20 deduced originally in Ref. 18.

For completeness, as demonstrated in Ref. 19, an H_2 subsidiary homoclinic orbit can be thought of as a primary homoclinic orbit. So, in general terms, we should find that there is a set of orbits H_{2nj} accumulating into a set H_{nj}, in a similar fashion that a subsidiary H_{2j} accumulates into a primary H_j. Thus, Fig. 3 shows a set of H_{4j} accumulating into H_{2j}, both subsidiaries of H_j.

To demonstrate that the scaling in Theorem 1 is also valid for this accumulation, we consider that, in the neighborhood of $\Delta\mu_j=0$, for $\Delta\mu_j\to\Delta\mu_{nj}$, $(r_{lnj},z_{lnj})=(r_{H_{nj}}+a\Delta\mu_{nj},m\Delta\mu_{nj})$ for $l=1$, where $\Delta\mu_{nj}=\mu-\mu_{nj}$ and $r_{H_{nj}}$ represents the coordinate r of the njth crossing of H_{nj} with the surface Σ_1. That conduces to equivalent solutions of Eq. (2) which results in the accumulation of H_{2nj} into H_{nj}. Since we

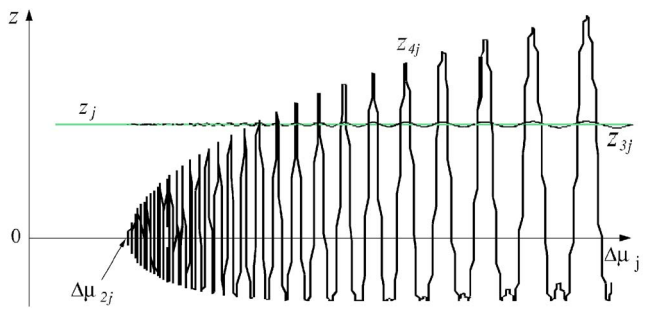

FIG. 3. A countable set of subsidiaries H_{4j} accumulating into a subsidiary H_{2j}. The z_{3j} curve is oscillating around the z_j curve. The z_{2j} is zero in $\Delta\mu_{2j}$ and cannot be distinguished by the axis $\Delta\mu_j$ in this scale. The subsidiary H_{2j} occurs in $\Delta\mu_{2j}$, indicated by the arrow. Parameters are the same presented in Fig. 2.

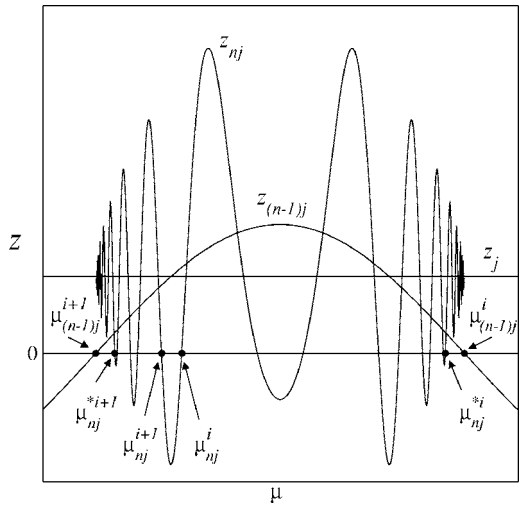

FIG. 4. We show the curves z_j, $z_{(n-1)j}$, and z_{nj}, and the parameters $\mu^{i+1}_{(n-1)j}$ and $\mu^{i}_{(n-1)j}$ corresponding to two consecutive subsidiary orbits $H^{i+1}_{(n-1)j}$ and $H^{i}_{(n-1)j}$. Likewise, μ^{i+1}_{nj} and μ^{i}_{nj} represent the parameters for which there are two consecutive subsidiary orbits H^{i+1}_{nj} and H^{i}_{nj}. The upper index $*k$ (with $k=\{i,i+1\}$) indicates the closest parameter μ_{nj} to $\mu^{i+1}_{(n-1)j}$ $(k=i+1)$ or to $\mu^{i}_{(n-1)j}$ $(k=1)$.

are considering $\Delta\mu_j \to 0$, the distribution and accumulations of homoclinic orbits, obtained by this analysis, also obeys Eq. (5). This shows that the scaling law predicted by Theorem 1 is valid for all subsidiary homoclinic orbits.

A. Estimation of the number of subsidiary homoclinic orbits

Knowing that the distribution of subsidiary homoclinic orbits obey the scaling law given by Eq. (5), we can improve our knowledge about the bifurcation of homoclinic orbits estimating the number of H_{nj} subsidiaries that exist between two consecutive $H_{(n-1)j}$ subsidiaries.

The inset of Fig. 2 shows that we can consider the z curve locally symmetric, which conduces to equivalent solutions of Eq. (3). Figure 4 illustrates a generic form of the z_{nj} solutions. In this figure the triangles formed by the vertices $[\mu^{i+1}_{(n-1)j}, \mu^{i+1}_{nj}, z^{i+1}_{(n-1)j}]$ and $[\mu^{i+1}_{(n-1)j}, \mu^{i}_{nj}, z^{i}_{(n-1)j}]$ can be considered approximately similar rectangular triangles, where the vertices $z^{i+1}_{(n-1)j}$ and $z^{i}_{(n-1)j}$ are points on the curve $z_{(n-1)j}$ for the parameters μ^{i+1}_{nj} and μ^{i}_{nj}, respectively. Therefore, we have that $\mu^{i}_{nj}-\mu^{i+1}_{(n-1)j}/\mu^{i+1}_{nj}-\mu^{i+1}_{(n-1)j}=z^{i}_{(n-1)j}/z^{i+1}_{(n-1)j}$ which equals the inverse of the right-hand side of Eq. (4), and therefore, we arrive at

$$\frac{\mu^{i}_{nj}-\mu^{i+1}_{(n-1)j}}{\mu^{i+1}_{nj}-\mu^{i+1}_{(n-1)j}} = e^{\lambda\pi/\omega}. \tag{6}$$

In order to estimate the number of subsidiary homoclinic orbits between two consecutive orbits, we consider the fact that the total number of elements of the geometric progression series $(a_i, a_{i+1}, \ldots, a_N)$, with $i=[1,2,3,\ldots,N]$ and ratio $q^{i-1}=a_i/a_1$, is given by

$$N = \frac{\ln(a_N/a_1)}{\ln(q)} + 1.$$

So, defining the first element a_1 to be the parameter distance $a_1=\mu^{*i+1}_{nj}-\mu^{i+1}_{(n-1)j}$, the last element $a_N=(\mu^{i}_{(n-1)j}-\mu^{i+1}_{(n-1)j})/2$, and the geometric ratio q given by Eq. (6), we estimate the number N of H_{nj} orbits within two consecutive $H_{(n-1)j}$ by $N=N^i+N^{i+1}$, where N^i is the number of orbits that appear in the right-hand side of the $z_{(n-1)j}$ curve (in Fig. 4) and N^{i+1} the number on the left-hand side. We find that

$$N^k = \left\{ \frac{\omega}{\lambda\pi} \ln \left| \frac{\mu^{i}_{(n-1)j}-\mu^{i+1}_{(n-1)j}}{2(\mu^{*k}_{nj}-\mu^{k}_{(n-1)j})} \right| + 1 \right\}, \tag{7}$$

where k represents either i or $i+1$ and the $\{\}$ operator implies that only the integer part of the right-hand side of Eq. (7) is taken.

We should expect that $N^i \neq N^{i+1}$. As the frequency of $z_{(n-1)j}$ increases for $z_{(n-2)j} \to 0$, the closer is one of the sides of the curve $z_{(n-1)j}$ to the orbit $H_{(n-2)j}$, the larger is the number of H_{nj} found. But, for the limit $z_j \to 0$, the difference between N^i and N^{i+1} is irrelevant compared to the total number N of orbits H_{nj}. At this situation, it is justified to consider that $N \cong 2N^k$ and, therefore, between two orbits $H_{(n-1)j}$ there are approximately $2N^k$ orbits H_{nj}.

III. HOMOCLINIC BIFURCATION IN THE CHUA'S CIRCUIT

To confirm our analytical findings, we use the Chua's circuit[12] whose rescaled equations are

$$\begin{aligned} \dot{x}' &= \alpha[y' - x' - k(x')], \\ \dot{y}' &= x' - y' + z', \quad \dot{z}' = -\beta y', \\ k(x') &= bx' + \tfrac{1}{2}(a-b)(|x'+1| - |x'-1|), \end{aligned} \tag{8}$$

and we set $a=-8/7$ and $b=-5/7$. α and β are control parameters.

The phase space of Eq. (8) has three domains: $D_0=\{\mathbb{R}^3 \| x' | \leqslant 1\}$, $D_+=\{\mathbb{R}^3 | x' \geqslant 1\}$, and $D_-=\{\mathbb{R}^3 | x' \leqslant -1\}$. There is a fixed point in each domain: $P_0=(0,0,0)$, in D_0, and $P_\pm=(\pm l, 0, \mp l)$, in $D_\pm$, where $l=(b-a)/(b+1)=1.5$. We focus our attention in homoclinic orbits to the saddle-focus point P_0. For this point, the Jacobian matrix of Eq. (8) has a pair of complex conjugate eigenvalues $-\rho \pm i\omega$ that determine the bidimensional stable subspace, $E^S(P_0)$, tangent to the stable manifold in the vicinity of P_0. It has also a real eigenvalue λ, that determines the one-dimensional subspace $E^U(P_0)$, which is tangent to the one-dimensional unstable manifold. A geometrical description of the Chua's circuit can be seen in Fig. 5; more details are in Ref. 26, where we have also described the conditions for the existence of a homoclinic orbit to the point P_0.

The relation between the coordinates used in Eq. (1), which led to the scaling in Eq. (5), and the coordinates used in Eq. (8) can be understood by the following analogy. The axis z, the plane W^S, Σ_0, and Σ_1 in Fig. 1 correspond to the unstable subspace $E^U(P_0)$, the plane $E^S(P_0)$, U_+, and a plane

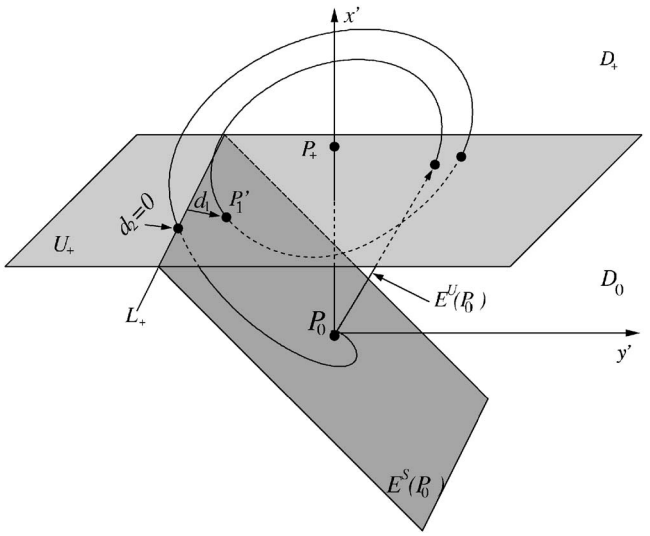

FIG. 5. Three-dimensional phase space of Eq. (8), with a slight rotation around the y' axis, for a better visualization. P_0 is the homoclinic orbit point and $E^S(P_0)$ and $E^U(P_0)$ are its stable and unstable subspaces, both limited by the plane $U_+=\{\mathbb{R}^3|x=+1\}$ which is the boundary of the domains D_0 with D_+. The distance between P_1', which is on the plane U_+, and the line $L_+ = E^S(P_0)\cap U_+$ is d_1. $d_2=0$, so there is a homoclinic orbit H_2, whose trajectory turns 2 times around the fixed point P_+.

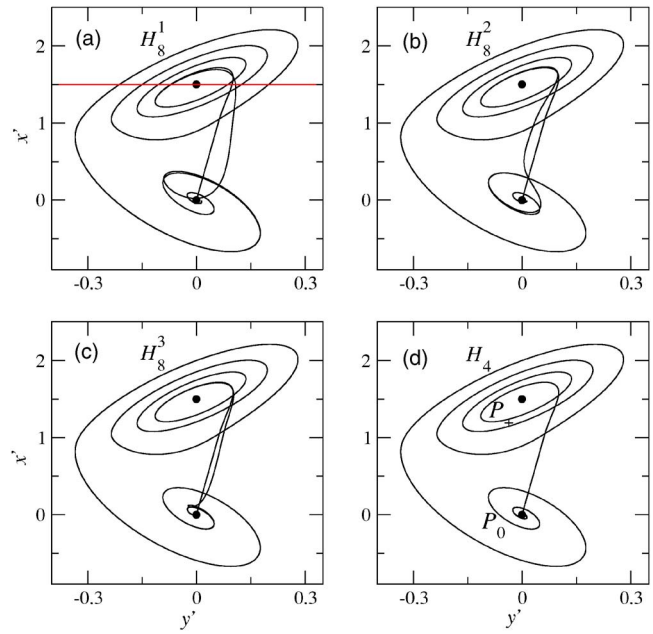

FIG. 6. Three subsidiary order-8 homoclinic orbits (a–c) in the vicinity of the order-4 primary (d) that appear for the parameters $\beta=52$ and $\alpha_8^1 = 23.639\,33$ (a), $\alpha_8^2=23.640\,35$ (b), $\alpha_8^3=23.640\,45$ (c), $\alpha_4=23.640\,51$ (d).

that contains $E^U(P_0)$ in Fig. 5, respectively. The distance d is linearly related to the z coordinate, used in Fig. 1, by a linear coefficient obtained from the relation between the (x',y',z') Chua's coordinates to the (x,y,z) theoretical coordinates.

In the proposed theory the order of a homoclinic orbit defines the number of times the point P_1 is mapped from Σ_0 to Σ_1, while for orbits in the Chua's circuit, the order defines the number of turns the orbit makes around the fixed point P_+. Both notions are equivalent in the sense that whenever, in this system, an orbit turns around the point P_+, there can almost always be found two planes Σ_0 to Σ_1, where similar mappings like Eqs. (2) exist. Numerically, finding an order-nj homoclinic orbit, H_{nj}, is equivalent to find a parameter set for which $d_{nj}=0$, with d_{nj} being the distance between the trajectory that leaves, $E^U(P_0)$ and turns nj times around P_+, and the line L_+ on the plane U_+, as represented in Fig. 5. (More details on the definition of d can be seen in Ref. 26.)

To illustrate the way we classify the homoclinic orbits, by specifying an order and whether or not it is a primary or subsidiary orbit, in Fig. 6 we show three order-8 subsidiary orbits (a–c) that appear in the vicinity of the order-4 primary (d). To determine the order of the orbit, i.e., how many times the orbit turns around the point P_+, indicated in (d), we count the number of times that the orbit crosses the line $x'=1.5$ [the x' coordinate of P_+ shown in (a)] in the direction where the x' coordinate is decrescent. Note that the subsidiary orbits preserve the form of the primary. In addition, as α_8^i approaches the parameter α_4, for which there is a primary H_4, the order-8 subsidiary orbits resembles more and more the primary. So, to discern if an order-k is a subsidiary orbit (k is an integer multiple of j), that accumulates/approaches into an order-j primary, or a primary orbit, one could simply note that the order-k subsidiary orbit would resemble the primary order-j orbit.

In order to extend the results in Eqs. (4) and (5) to the Chua's circuit, we put Eq. (4) in terms of the distances d. As previously discussed, the d_{nj} curve is linearly related with the z_{nj} curve, so

$$d_{nj} = Cz_{nj}, \tag{9}$$

with C being a term that slowly varies in a linear rate proportional to $\Delta\alpha_j=\alpha-\alpha_j$ and thus it is treated as a constant. That implies that for small $\Delta\alpha_j$,

$$\frac{d_{(n-1)j}^{i+1}}{d_{(n-1)j}^{i}} = e^{-\lambda\pi/\omega}.$$

This equation lead us to a scaling for the parameter distance $\Delta\alpha_j=\alpha_{nj}-\alpha_j$ of subsidiary homoclinic orbits of order nj in the vicinity of primaries of order j

$$S = \frac{\alpha_{nj}^{i}-\alpha_{nj}^{i+1}}{\alpha_{nj}^{i-1}-\alpha_{nj}^{i}}. \tag{10}$$

For larger i values, $\Delta\alpha_j$ decreases, and the scaling S should converge to the one in Eq. (5), $S_T=e^{-\lambda\pi/\omega}$. Although this scaling law was derived for smooth systems, it is also valid for the non smooth Chua's circuit because near the fixed point P_0 the differential equations (8) are smooth. Moreover, for the Chua's circuit, the surfaces Σ_0 and Σ_1 (defined for the mappings used to derive the scaling law) are inside one domain (D_0), for which the system is linear, i.e., smooth.

In the parameter space of Fig. 7(a) primary homoclinic orbit bifurcations are identified. Except for the H_1 bifurcation line, all the other bifurcation lines (orders varying from 2 to 7) have two branches, left and right, as indicated for the H_7 curve. For parameters within a region bounded by a bifurcation line $d_j<0$ and, therefore, no subsidiary orbits are found. That is shown in Fig. 7(b) for $\beta=8.8$, where it is shown the

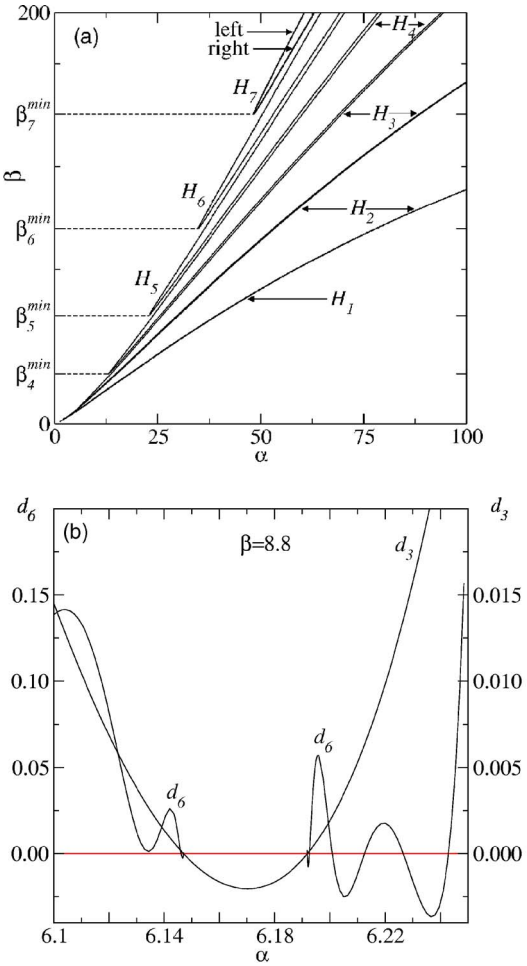

FIG. 7. (a) Parameter space of the primary homoclinic orbits H_n, with $n=1,\ldots,7$. (b) Accumulation of subsidiaries H_6 ($d_6=0$) into two primaries H_3 ($d_3=0$) for $\beta=8.8$. The vertical axis shows on the left side the value of d_6 and on the right side the value of d_3. $\beta_j^{\min}$ represents the minimum β value for a given H_j.

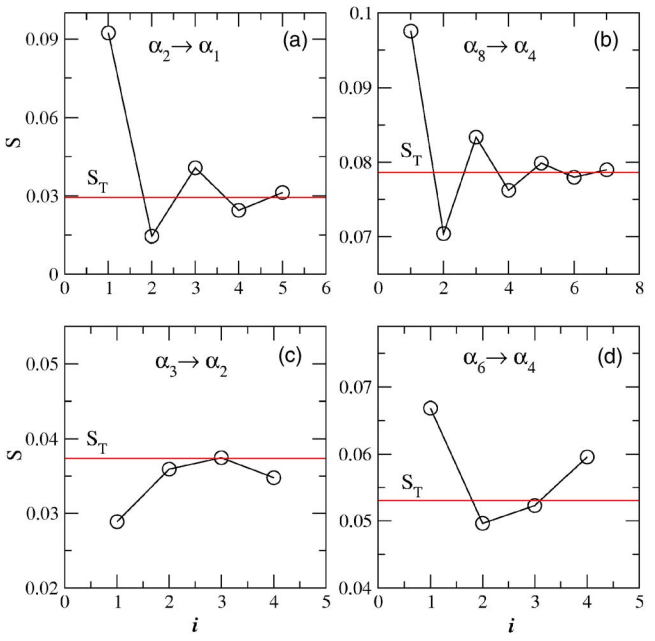

FIG. 8. The scaling $S=\alpha_{nj}^i-\alpha_{nj}^{i+1}/\alpha_{nj}^{i-1}-\alpha_{nj}^i$ of the approach of H_{nj} into the $H_{(n-1)j}$ homoclinic orbit, for $j=1$, $n=2$, and $S_T=e^{-\lambda\pi/\omega}=0.0293$ (a), $j=4$, $n=2$, and $S_T=0.0786$ (b), $j=1$, $n=3$, and $S_T=0.0374$ (c), and $j=2$, $n=3$, and $S_T=0.0594$ (d).

accumulation of subsidiaries H_6 into two primaries H_3 by the left and right sides. Within the α interval where $d_3<0$, there are no H_{nj} homoclinic orbits. These orbits appear between the right branch of an order-$(j+1)$ primary orbit and the left branch of an order-j primary orbit. A complete picture and topology analysis of this microscopic character of the homoclinic bifurcation scenario in the Chua's circuit can be seen in Ref. 23.

An example of the relation between the existence of homoclinic orbits and fundamental properties and bifurcations in the Chua's circuit can be seen in Fig. 7(a). In this figure, $\beta_j^{\min}$ represents the minimum β value for a given H_j. The resulting curve connecting all the minimum parameter values $(\alpha,\beta_j^{\min})$, for which primary homoclinic orbit exist, is very close to the crisis line in which the Rössler-type attractor bifurcates into the Double Scroll attractor through a crisis-induced intermittency.[30] So, this crisis should be associated with the creation of an infinite number of homoclinic orbits and therefore, an infinite number of horseshoes.

In Figs. 8(a)–8(d) we show a series of pictures showing the approach of H_{nj} homoclinic orbits into the orbit $H_{(n-1)j}$. This scaling constitutes the characterization of the microscopic structure of the homoclinic bifurcation scenario in the bidimensional parameter space of the Chua's circuit. In the vertical axis we show S determined by Eq. (10). The line represents the value S_T, with λ and ω calculated for parameters of the primary homoclinic orbits. Figures 8(a) and 8(b) show the scaling of the approach of subsidiaries H_{2j} into primaries H_j. In (a) the primary H_1 appears for $\alpha_1=2.758\,67$ and $\beta=3$, while in (b) the primary H_4 appears for $\alpha_4=23.640\,51$ and $\beta=52$. The approach of subsidiaries H_{nj} into subsidiaries $H_{(n-1)j}$ is shown in Figs. 8(c) and 8(d). In (c), H_3 approaches into H_2 ($\alpha_2=6.199\,62$, $\beta=7.5$), in the vicinity of the primary H_1 ($\alpha_1=6.199\,66$, $\beta=7.5$), and in (d) H_6 approaches into H_4 ($\alpha_4=15.400\,64$, $\beta=25$), in the vicinity of the primary H_2 ($\alpha_2=15.405\,98$, $\beta=25$). Note that the scaling with which parameters of subsidiary orbits accumulate/approach into H_4 in (b) and (d) are far away from the parameter for which the primary H_1 appears, and therefore, it is clear the validity of the Theorem 1 for extended regions in the parameter space. While the scaling S converges to S_T for accumulations of subsidiaries into the primaries, as i grows [Figs. 8(a) and 8(b)], for the approaching of subsidiaries into subsidiaries, the theoretical ratio S_T gives a good estimation of the obtained S values [Figs. 8(c) and 8(d)]. It reflects the fact that there is no accumulation of subsidiaries H_{nj} into subsidiaries $H_{(n-1)j}$ because, in this region, there is a finite number of H_{nj}. Nevertheless, there is an infinite number of H_{sj}, with $s>n$.

A. Estimation of the number of subsidiary orbits in the Chua's circuit

In the following, we show that the number of subsidiary orbits between subsidiary orbits can be estimated by

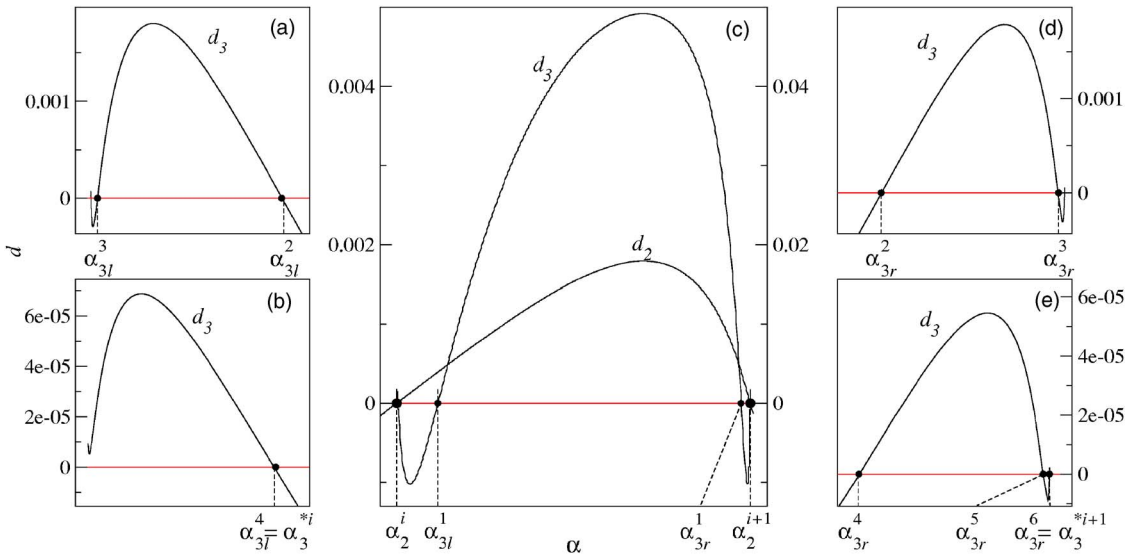

FIG. 9. Curves d_2 and d_3. (a–b) are successive magnifications of (c) in the region close to the parameter α_2^i=6.199 620 571 935 for which there is a subsidiary H_2 orbit (filled circle in the left of the figure). (d–e) are successive magnifications of (c) in the region close to the parameter α_2^{i+1}=6.199 654 388 756 for which there is a subsidiary H_2 orbit (filled circle in the right of the figure). The leftmost H_3 orbit appears for the parameter α_3^{*i}=6.199 620 572 167 indicated in (b) and the rightmost H_3 orbit appears for the parameter α_3^{*i+1}=6.199 654 388 755. In (c) the left and the right vertical axes indicate the values of the d_2 and d_3 curves, respectively. The indices l and r differentiate the left series (crescent d_2 function) to the right series (decrescent d_2 function) of α_3^i.

$$N^k = \left\{ \frac{\omega}{\lambda \pi} \ln \left| \frac{\alpha^i_{(n-1)j} - \alpha^{i+1}_{(n-1)j}}{2(\alpha^{*k}_{nj} - \alpha^k_{(n-1)j})} \right| + 1 \right\}, \tag{11}$$

where $\alpha_{nj}^{*k=i}$ represent the parameter of the closest subsidiary H_{nj} to the subsidiary $H^i_{(n-1)j}$, and $\alpha_{nj}^{*k=i+1}$ the parameter of the closest subsidiary H_{nj} to $H^{i+1}_{(n-1)j}$ [and therefore closer to the orbit $H_{(n-2)j}$]. N^k is the estimated number of orbits H_{nj} approaching into $H^i_{(n-1)j}$ $(k=i)$ or into $H^{i+1}_{(n-1)j}$ $(k=i+1)$. To derive Eq. (11) we have used Eq. (9) in Eq. (7).

Figure 9 shows the distribution of the subsidiary H_3 orbits within two consecutive subsidiary H_2, in the vicinity of a primary H_1 orbit. Using the α parameter values indicated in the caption of Fig. 9, and the fact that $e^{\lambda\pi/\omega}=1/0.0374$, we can estimate the number of orbits H_3 that appear for parameters for which the d_2 curve is crescent $(k=i)$ and decrescent $(k=i+1)$. We arrive that $N^i=4$ and $N^{i+1}=6$, which is exactly the number of orbits observed in our simulations. So, the number of orbits from the left side of the crescent d_2 function is lower than the number of orbits from the right side of the decrescent d_2 function.

IV. CONCLUSION

In conclusion, it has been known that homoclinic orbits bifurcate in dynamical systems that have saddle-focus points, when the condition of Shilnikov is satisfied.[14,18] Here, a scenario of these bifurcations was demonstrated in the neighborhood of any primary homoclinic orbit H_j $(j \in \mathbb{N})$. In Ref. 18 a scaling law was derived for H_2 accumulating in H_1 homoclinic orbits. Here, we derived an exponential scaling law that describes the parameter distribution of general sets of subsidiary homoclinic orbits H_{nj} $(n \geqslant 2)$ near the parameter for which primary homoclinic orbits H_j exists. As it was discussed in Sec. II, our result is in agreement with Refs. 16 and 20 and it was verified by either calculating the distribution of subsidiary homoclinic orbits in the vicinity of a primary one, in the Chua's circuit, or by predicting the number of subsidiary H_{nj} orbits that appear between a pair of consecutive $H_{(n-1)j}$ subsidiary homoclinic orbits, in the vicinity of a H_j. Moreover, one can consider any subsidiary as a primary orbit with families of subsidiary orbits distributed nearby with the same scaling law.

A relevant achievement in this work was to show that the proposed scaling is valid in the neighborhood of any primary homoclinic orbit, and the prediction clearly demonstrated to be valid in the parameter space of the homoclinic bifurcation in the Chua's circuit. The fact that this scaling is valid everywhere in this parameter space has a great experimental appeal, since an experimentalist is not restricted to looking for homoclinic orbits in a particular range of parameters, but is free to use possible accessible parameters, available in the experiment.

Whenever there is a Shilnikov homoclinic orbit, there is an infinite number of periodic orbits and horseshoes associated with it.[25] Therefore, an infinite number of periodic orbits and complex horseshoes will be found following the same parameter scaling laws derived in this work. As discussed in Ref. 18 the presented scaling should be also valid for higher dimensional systems.

These results indicate how sensitive the system is to even small changes of the control parameters, and, furthermore, they can be used to determine critical regions in the parameter space where attractor bifurcations occur. Thus, our approach, using Shilnikov's theorem to understand how Shilnikov orbits are created, may contribute to understanding the relation between homoclinic Shilnikov orbits and bifurcations in chaotic attractors.

Our analytical findings are valid for systems whose dynamical behavior in the vicinity of the saddle-focus point are given by a linear transformation. It remains to be seem to

which class of dynamical systems this linear transformation succeeds in describing their homoclinic bifurcation scenario.

ACKNOWLEDGMENTS

We thank the financial support of FAPESP and CNPq. M.S.B acknowledges the financial support of the Alexander von Humboldt Foundation and Helmholz Center for the Brain and Mind.

[1]D. Auerbach, P. Cvitanović, J. P. Eckmann, G. Gunaratne, and I. Procaccia, "Exploring chaotic motion through periodic orbits," Phys. Rev. Lett. **58**, 2387 (1987); M. H. Jensen, L. P. Kadanoff, and I. Procaccia, "Scaling structure and thermodynamics of strange sets," Phys. Rev. A **36**, 1409 (1987); G. H. Gunaratne and I. Procaccia, "Organization of chaos," Phys. Rev. Lett. **59**, 1377 (1987); P. Cvitanović, "Invariant measurement of strange sets in terms of cycles," *ibid.* **61**, 2729 (1988); O. Biham and W. Wenzel, "Characterization of unstable periodic orbits in chaotic attractors and repellers," *ibid.* **63**, 819 (1989); C. Grebogi, E. Ott, and J. A. Yorke, "Unstable periodic orbits and the dimension of chaotic attractors," Phys. Rev. A **36**, 3522 (1987); **37**, 1711 (1988).

[2]S. Smale, *Differential and Combinatorial Topology* (Princeton University Press, Princeton, 1963); S. Smale, Bull. Am. Math. Soc. **73**, 747 (1967).

[3]L. P. Shilnikov, "A case of the existence of a countable number of periodic motions," Sov. Math. Dokl. **6**, 163 (1965); "On the generation of periodic motion from trajectories doubly asymptotic to an equilibrium state of a saddle type," Math. USSR. Sb. **6**, 427 (1968); **10**, 91 (1970).

[4]P. Coullet, C. Tresser, and A. Arneodo, "Transition to stochasticity for a class of forced oscillators," Phys. Lett. **72**, 268 (1979); A. Arneodo, P. Coullet, E. A. Spiegel, and C. Tresser, "Asymptotic chaos," Physica D **14**, 327 (1985); F. Argoul, A. Arneodo, and P. Richetti, "Experimental evidence for homoclinic chaos in the Belousov-Zhabotinskii reaction," Phys. Lett. A **120**, 269 (1987); F. Argoul, A. Arneodo, P. Richetti, J. C. Roux, and H. L. Swinney, "Chemical chaos: From hints to confirmation," Acc. Chem. Res. **20**, 436 (1987).

[5]F. T. Arecchi, A. Lapucci, R. Meucci *et al.*, "Experimental Characterization of Shilnikov chaos by statistics of return times," Europhys. Lett. **6**, 677 (1988); F. T. Arecchi, R. Meucci and W. Gadomski, "Laser dynamics with competing instabilities," Phys. Rev. Lett. **58**, 2205 (1987).

[6]T. Braun, J. A. Lisboa, and J. A. C. Gallas, "Evidence of homoclinic chaos in the plasma of a glow discharge," Phys. Rev. Lett. **68**, 2770 (1992).

[7]E. M. Izhikevich, "Neural excitability, spiking and bursting," Int. J. Bifurcation Chaos Appl. Sci. Eng. **10**, 1171 (2000).

[8]U. Feudel, A. Neiman, X. Pei *et al.*, "Homoclinic bifurcation in a Hodgkin-Huxley model of thermally sensitive neurons," Chaos **10**, 231 (2000).

[9]D. Parthimos, D. H. Edwards, and T. M. Griffith, "Shilnikov homoclinic chaos is intimately related to type-III intermittency in isolated rabbit arteries: Role of nitric oxide," Phys. Rev. E **67**, 051922 (2003).

[10]C. S. Zhou, J. Kurths, E. Allaria *et al.*, "Constructive effects of noise in homoclinic chaotic systems," Phys. Rev. E **67**, 015205 (2003).

[11]M. T. M. Koper, P. Gaspard, and J. H. Sluyters, "Mixed-mode oscillations and incomplete homoclinic scenarios to a saddle focus in the indium/thiocyanate electrochemical oscillator," J. Chem. Phys. **97**, 8250 (1992).

[12]T. Matsumoto and L. O. Chua, "The double scroll," IEEE Trans. Circuits Syst. **CAS-32**, 797 (1985).

[13]The Shilnikov condition for a three-dimensional system is $|\rho/\lambda|<1$, where λ is one real eigenvalue and ρ is the real part of the other two complex conjugate eigenvalues.

[14]S. Hasting, "Single and multiple pulse waves for the FitzHugh-Nagumo," SIAM J. Appl. Math. **42**, 247 (1982).

[15]J. W. Evans, N. Fenichel, and J. A. Feroe, "Double impulse solutions in nerve axon equations," SIAM J. Appl. Math. **42**, 219 (1982).

[16]P. Glendinning and C. Sparrow, "Local and global behavior near homoclinic orbits," J. Stat. Phys. **35**, 645 (1984); P. Glendinning and C. Laing, "A homoclinic hierarchy," Phys. Lett. A **211**, 155 (1996).

[17]S. Wiggins, *Introduction to Applied Nonlinear Dynamical Systems and Chaos* (Springer, New York, 1996).

[18]P. Gaspard, "Generation of a countable set of homoclinic flows through bifurcation," Phys. Lett. **97**, 1 (1983); P. Gaspard, R. Kapral, and G. Nicolis, "Bifurcation phenomena near homoclinic systems: A two-parameter analysis," J. Stat. Phys. **35**, 697 (1984).

[19]J. A. Feroe, "Homoclinic orbits in a parametrized saddle-focus system," Physica D **62**, 254 (1993).

[20]S. V. Gonchenko, D. V. Turaev, P. Gaspard, and G. Nicolis, "Complexity in the bifurcation structure of homoclinic loops to a saddle-focus," Nonlinearity **10**, 409 (1997).

[21]P. Gaspard and G. Nicolis," What can we learn from homoclinic orbits in chaotic dynamics," J. Stat. Phys. **31**, 499 (1983).

[22]S. V. Gonchenko, L. P. Shilnikov, and D. V. Turaev, "On models with non-rough Poincaré homoclinic curves," Physica D **62**, 1 (1993); S. V. Gonchenko, D. V. Turaev, and L. P. Shilnikov, "Dynamical phenomena in multi-dimensional systems with a non-rough Poincaré homoclinic curves," Dokl. Akad. Nauk **330**, 144 (1993).

[23]R. O. Medrano-T., M. S. Baptista, and I. L. Caldas, "Basic structures of the Shilnikov homoclinic bifurcation scenario," Chaos **15**, 033112 (2005).

[24]S. Kahan and A. C. Sicardi-Schifino, "Homoclinic bifurcations in Chua's circuit," Physica A **262**, 144 (1999).

[25]T. Matsumoto, M. Komuro, H. Kokubu, and R. Tokunaga, *Bifurcations: Sights, Sounds, and Mathematics* (Springer, New York, 1993).

[26]R. O. Medrano-T., M. S. Baptista, and I. L. Caldas, "Homoclinic orbits in a piecewise system and its relations with invariant sets," Physica D **186**, 133 (2003).

[27]I. M. Ovsyannikov and L. P. Shilnikov, "Systems with a homoclinic curve of multidimensional saddle-focus type, and spiral chaos," Math. USSR. Sb. **73**, 415 (1992); **130**, 557 (1996).

[28]B. Deng, "The Shil'nikov problem, exponential expansion, strong λ-lemma, C^1-linearization, and homoclinic bifurcations," J. Differ. Equations **79**, 189 (1989); C. Robinson, "Homoclinic bifurcation to a transitive attractor of Lorenz type," Nonlinearity **2**, 495 (1989); M. Rychlik, "Lorenz attractor through Shilnikov type bifurcation," Ergod. Theory Dyn. Syst. **10**, 793 (1990); D. V. Turaev and L. P. Shilnikov, "An example of a wild strange attractor," Sitzungsber. Preuss. Akad. Wiss., Phys. Math. Kl. **189**, 291 (1996).

[29]In the case one wants to demonstrate the infinite number of periodic orbits in the neighborhood of a primary homoclinic orbit H_j, following the steps in the Shilnikov Theorem, one should use Eqs. (2) for $n>1$ with the condition that $r_{nj}=r_{(n-1)_j}$ and $z_{nj}=z(n-1)_j$. As they stand, these equations give the crossings of the unstable manifold (for an inverse time) of the point P_0, along the surface Σ_1, starting from the special point P_1 on the surface Σ_0. Therefore, Eqs. (2) are not equations for periodic orbits, but for the unstable manifold of the equilibrium point P_0.

[30]C. Grebogi, E. Ott, F. Romeiras *et al.*, "Critical exponents for crisis-induced intermittency," Phys. Rev. A **36**, 5365 (1987).